

Evaluation of the Glass Transition Temperature and Intermolecular Interaction of Poly(ethylene oxide) with Addition of Lithium Perchlorate or/and Titanium Dioxide

S.N.H.M. Yusoff^{1,*}, N.F.A. Zainal²

¹Faculty of Applied Sciences, Universiti Teknologi MARA Cawangan Johor Kampus Pasir Gudang, 81750 Masai, Johor, Malaysia.

²Centre of Foundation Studies, Universiti Teknologi MARA, Cawangan Selangor Kampus Dengkil, 43800 Dengkil, Selangor, Malaysia

*Corresponding author: sitiinorhafiza@uitm.edu.my

Article history:

Received 01 September 2024

Accepted 30 October 2024

ABSTRACT

The high crystallinity of poly(ethylene oxide) (PEO) has urged the need for adding salt or nanofiller to explore the electrochemical performance of solid polymer electrolytes (SPEs). The effect of the glass transition temperature (T_g) and intermolecular interaction of PEO upon the addition of salt or nanofiller has become a debatable topic due to the lack of understanding of the role of salt or nanofiller in PEO. Hence, the evaluation of the T_g and intermolecular interaction of PEO with the addition of lithium perchlorate (LiClO_4) salt or/and titanium dioxide (TiO_2) nanofiller is presented and discussed. The solid polymer electrolytes with the addition of nanofiller are prepared by solution casting technique. The optimum composition of PEO and LiClO_4 salt is used as the host matrix and TiO_2 as the nanofiller. The T_g and intermolecular interaction of the polymer-based electrolytes have been studied by Differential Scanning Calorimeter (DSC) and Fourier Transform Infrared spectroscopy (FTIR), respectively. PEO- LiClO_4 serves as the classical model of polymer-salt systems with good polymer-salt molecular interaction at low salt concentrations ($W_s \leq 0.107$) whereas TiO_2 without any surface treatment when added to PEO, serves as a classical model of polymer-nanofiller systems with weak polymer-nanofiller molecular interaction. Results have shown that LiClO_4 salt has a notable effect on the T_g and intermolecular interaction of PEO. Whereas, TiO_2 does not provide a substantial effect on the T_g and intermolecular interaction of PEO-based polymer electrolytes. This work provides a better understanding and knowledge of the effect of the addition of salt or/and nanofiller in the T_g and intermolecular interaction of the PEO systems.

Keywords: intermolecular interaction, glass transition temperature (T_g), poly(ethylene oxide), lithium perchlorate, titanium dioxide

© 2024 Faculty of Chemical and Engineering, UTM. All rights reserved

| eISSN 0128-2581 |

1. INTRODUCTION

Solid polymer electrolytes (SPE) have garnered significant interest in recent decades owing to their potential applications in solid-state batteries, fuel cells, supercapacitors, sensors and etc. [1–9]. SPE is prepared by dissolving the alkali metal salt in a polymer host [10–12]. These electrolytes provide several appealing benefits compared to their liquid counterparts, including leakage-free, safe, lightweight, and easy to synthesize in desirable thickness and area [2,13]. PEO-based solid polymer electrolyte is extensively studied due to its lower lattice energy [14], high solvating power for alkali metal salts [15], good electrochemical stability [16], and appropriate structure for facilitating rapid ion transport [17]. PEO contains Lewis base ether oxygen, which coordinates with the cations and thus helps to dissolve the inorganic salts

[1,17,18]. The main drawback of PEO-based solid polymer electrolyte is its high crystalline phase below the melting temperature which renders it unsuitable for application in batteries or other practical electrochemical devices. It has been revealed that the neat semicrystalline PEO has ~70% of the crystalline phase [19,20].

To address this issue, researchers have explored various strategies to enhance the overall performance of PEO-based electrolytes. These strategies include the incorporation of plasticizers to disrupt the crystalline structure [21,22], the use of nanofillers to enhance ion transport pathways [23,24], and the optimization of polymer-salt interactions. Furthermore, advances in material processing techniques and composite formulations are being investigated to reduce the crystallinity and improve the electrochemical properties of PEO-based electrolytes. Ongoing research aims to balance the mechanical stability,

ionic conductivity, and thermal stability of these materials, paving the way for their broader application in next-generation energy storage and conversion technologies.

For concept-proof, a lithium salt is chosen to be added to the PEO matrix for the application of SPE due to the high solvating property of PEO with the inorganic salt [11,25]. However, due to the high crystallinity of PEO, this may limit the application of the binary mixture of PEO with a salt as SPE [26]. The dissolution of salt only occurs in the amorphous region of the polymer matrix, where it plays the percolation pathway for the conductivity of dipolar entities of salt and PEO [27]. Meanwhile, inert nanofiller titanium dioxide (TiO₂) may offer excellent characteristics for the improvement of lithium-ion batteries [22,28,29]. However, inconsistent implications were deduced from the previous studies on how the nanofiller affects the properties and enhances the conductivity of the SPEs [30,31]. To date, the correlation of T_g-intermolecular interaction is crucial for regulating the performance of SPEs especially on the molecular interaction between the active surface of the nanofiller and the polymer chains, for which this attributing factor may be oversimplified [32,33].

Since there are limited reports on the effects of the addition of nanofiller into the SPEs that may lead to an enhancement in their performance for applications in batteries and other electrochemical devices, this work will explore the relationship between thermal properties and intermolecular interactions when PEO is added with salt and/or nanofillers. Differential Scanning Calorimeter (DSC) and Fourier Transform Infrared spectroscopy (FTIR) technique is employed to study the glass transition temperature (T_g) and to elucidate specific polymer-salt, polymer-nanofiller and polymer-salt-nanofiller intermolecular interaction of PEO with the addition of salt or/and nanofiller, respectively [34,35]. This will include a detailed discussion on the shifting of wavenumbers, changes in band shapes and intensities, and alterations in other band properties. The T_g of PEO and its molecular interactions with salts and nanofillers play crucial roles in determining the performance of PEO-based solid polymer electrolytes. By understanding and manipulating these factors, researchers can design electrolytes with optimized properties for various applications in energy storage and conversion technologies.

2. EXPERIMENTAL SECTION

2.1 Materials

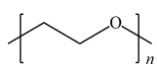
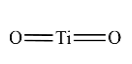
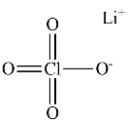
Three systems, *i.e.*, (1) polymer-salt, (2) polymer-nanofiller and (3) polymer-salt-nanofiller systems were studied in this work. PEO as the polymer host, LiClO₄ as the salt, and TiO₂ as the nanofiller were employed in this work. In this work, the rutile form of TiO₂ with a particle size of < 100 nm (99.5% trace metal basis) was selected due to its structural stability at various temperatures, high chemical stability, excellent optical transparency [36] and more surface active than other fillers [2,37] which offers various

fields of potential applications for example photocatalysis [38], pharmaceuticals [39], electronic devices [40], *etc.* Therefore, TiO₂ was chosen as the conceptual model for this study in order to explore the effect of incorporating TiO₂ into a polymeric system. This will facilitate a more comprehensive understanding of the applicability of TiO₂ to be used as a nanofiller in polymeric systems.

PEO was purified by dissolution in chloroform (CHCl₃) (Merck, Darmstadt, Germany) and precipitation in *n*-hexane (Merck, Darmstadt, Germany) before the addition of salt or nanofiller. The salt and nanofiller were dried at 120 °C for at least 24 h prior to sample preparation. The characteristics of the polymer, salt, and nanofiller used in this work are tabulated in

Table 1.

Table 1. Characteristics of materials used in this work

Constituent	PEO	TiO ₂	LiClO ₄
M_n^a (g mol ⁻¹)	300,000	-	-
M_w^b (g mol ⁻¹)	-	79.87	106.4
T_m (°C)	65 ^c	-	236 ^d
T_g^e (°C)	-53	-	-
Molecular structure			
Supplier	Sigma-Aldrich (St. Louis, MO, USA)	Sigma Aldrich Chemical Co. (USA)	Acros Organics Co, Geel, Antwerp, Belgium

^aViscosity-average molar mass estimated by the supplier;

^bMolar mass calculated by the supplier; ^cMelting temperature adapted from ref [19]; ^dMelting temperature adapted from ref [41]; ^eGlass transition temperature estimated from DSC as determined in this work

2.2 Sample Preparation

A solution-casting technique was used to prepare the free-standing polymer-salt, polymer-nanofiller and polymer-salt-nanofiller films. The PEO was added with different salt fraction (W_S) in the range of 0 to 0.17, or nanofiller fraction (W_F) in the range of 0 to 0.065 for preparation of polymer-salt or polymer-nanofiller films, respectively. The equation to determine the mass fraction of salt and nanofiller is as follows

$$W_i = \frac{m_i}{m_{PEO} + m_i} \quad (1)$$

where quantity m_i and m_{PEO} represent the mass of component i and PEO, respectively. The component i can be noted as the salt or nanofiller used in this work. For polymer-salt systems, the PEO was dissolved in tetrahydrofuran (THF)

(Merck, Darmstadt, Germany) and was stirred for at least 24 h at 50 °C. The polymer-salt mixture was poured onto the Teflon dish and was left to dry without undergoing extra stirring. Unlike the polymer-salt mixture, the polymer-nanofiller system was dissolved in acetonitrile (ACN) (Merck, Darmstadt, Germany) and was stirred for at least 24 h at 50 °C. ACN was used to prepare the polymer-nanofiller solutions due to the higher polarity and interaction of ACN, which promotes better dispersion of a highly agglomerated TiO₂ filler in the polymer solution. Further stirring using T18D Ultra-Turrax homogenizer (IKA, Stauffer, Germany) for 15 min at a speed of 5000 rpm was done for the polymer-nanofiller mixture in order to reduce the agglomeration of the nanofiller. Meanwhile, for the preparation of polymer-salt-nanofiller systems, the composition of salt is fixed based on the optimum composition of salt obtained from the polymer-salt system (*i.e.*, $W_S = 0.107$) with increasing nanofiller fraction (W_F) in the range of 0 to 0.043. The range of composition of nanofiller before the agglomeration of nanofiller (*i.e.*, obtained from polymer-nanofiller systems). The polymer-salt-nanofiller system was dissolved in ACN and was stirred for at least 24 h at 50 °C and further stirred using homogenizer for another 15 min at a speed of 5000 rpm.

Then, the polymer-salt, polymer-nanofiller and polymer-salt-nanofiller mixture was poured slowly onto the Teflon dish and left to evaporate until a dried film was formed. After drying, all systems were heated at 80 °C under a nitrogen atmosphere for 30 min (to erase the thermal history during the sample preparation) before being further dried in a vacuum oven for 24 h at 25 °C. All samples were kept in desiccators before further characterization.

2.3. Instruments

2.3.1 Differential Scanning Calorimetry (DSC)

Thermal properties of polymer-salt, polymer-nanofiller and polymer-salt-nanofiller systems were studied using DSC TA Q200 (TA Instrument, New Castle, USA) equipped with RCS90 cooling system (TA Instrument, New Castle, USA). Before the analysis, calibration using indium and sapphire standards was done. Around 10 to 15 mg of the sample was used for each analysis. The sample was placed in a standard aluminium sample pan (*i.e.*, sealed hermetic pan) before starting the thermal procedure for DSC analysis. The sample was cooled to -90 °C and heated up to 80 °C at a rate of 10 °C min⁻¹. Nitrogen gas was purged throughout the analysis at a rate of 50 mL min⁻¹ to avoid the thermo-oxidative degradation of the sample in the DSC furnace. The quantity of T_g of the sample was extracted from the first heating cycle of DSC thermogram. The T_g was extrapolated at the mid-point of the change in heat capacity (ΔC_p) or by using Moynihan's method for a more precise estimation of T_g especially for the sample with the existence of relaxation endotherm in the glass transition[42–44]

2.3.2 Fourier Transform Infrared (FTIR)

The intermolecular interactions of the film samples with a thickness of 0.2 – 0.4 mm were examined by FTIR spectroscopy. The FTIR spectrum of each polymer-salt, polymer-nanofiller and polymer-salt-nanofiller systems were recorded using an attenuated total reflectance (ATR) accessory with a diamond crystal window on Nicolet iS10 FTIR (Thermo Scientific, Madison, Wisconsin, USA). The dried film was pressure-clamped to ensure that the film was in adequate contact with the ATR crystal. The spectra were collected in absorbance mode in the range of wavenumber 600 - 4000 cm⁻¹ by averaging 16 scans at a maximum resolution of 2 cm⁻¹ at 25 °C. The sample was analyzed at three locations with a minimum of six FTIR measurements to ensure that the FTIR analysis was based on a representative region of the polymer-salt, polymer-nanofiller and polymer-salt-nanofiller systems, respectively. The spectrum obtained was subjected to background subtraction and auto-baseline correction to attain the final spectrum.

3. RESULTS AND DISCUSSION

3.1 Glass Transition Temperature

T_g is one of the important properties of polymers, which describes the temperature at which the polymer chains start to move. Below T_g , the polymer chains are rigid and have very little mobility. The T_g is influenced by the molecular structure of polymers [45,46], molar mass [44,47], crystallinity and thermal history [48]. Lowering the T_g can increase the polymer chains' mobility and consequently increase the conductivity [49,50]. This is due to the enhanced flexibility of the polymer chains and faster segmental motion. Since the conductivity of SPEs at room temperature is still low, strategies have been conducted in an attempt to lower the T_g far below room temperature and enhance the conductivity.

Figure 1 shows the T_g of amorphous PEO for PEO-LiClO₄, PEO-TiO₂ and PEO-LiClO₄-TiO₂ systems. There is a linear increase in T_g with elevating salt content up to $W_S = 0.0909$ for the PEO-LiClO₄ systems but not in the PEO-TiO₂ and PEO-LiClO₄-TiO₂ systems. This shows that the salt has a significant effect on the amorphous region of the semicrystalline PEO than the nanofiller. In other words, the salt possesses better interaction with PEO than the nanofiller. One can see that the variation in T_g for the polymer-based nanofiller systems is insignificant as each T_g -nanofiller composition is within the percentage error. Besides, it is also well-known that the salt is more soluble in PEO, unlike the ceramic nanofiller, where phase separation takes place in the binary (or ternary) mixture, even with surface modification of the nanofiller [51–55]. This is because the ceramic nanofiller does not dissolve in the polymer.

It can be seen that PEO-LiClO₄ systems are only miscible up to a certain composition as the T_g increase linearly up to saturation point ($W_S > 0.107$), before it drops until reaching near the T_g of neat PEO (T_g^0), indicating the occurrence of phase separation in the amorphous region. In

other words, above the saturation point at $W_s > 0.107$, PEO-LiClO₄ systems undergo a phase separation forming the salt-rich and salt-poor phases. Salt-rich and salt-poor phases refer to the pure salt phase (salt precipitation due to excessive amount of salt in PEO) and the phase of highly diluted salt solution in the PEO, respectively. This phase can be observed from the micrograph from the polarized optical microscope (POM) that has been reported in previous work [20,56]. It is well noted that an increase in T_g elucidates the increase in rigidity of the polymer chain, which may also imply the interaction between the constituents in the mixture [57–59]. Hence, from the presented data, the increase in T_g observed in PEO-LiClO₄ systems implies the interaction between PEO and LiClO₄ salt. Consequently, it leads to a decrease in the degree of freedom of molecular chains of PEO with elevating salt fraction unlike the TiO₂ nanofiller, where little to no effect on the degree of freedom of PEO chains. This observation is absent for the PEO-TiO₂ and PEO-LiClO₄-TiO₂ systems which expresses the immiscibility of TiO₂ and PEO.

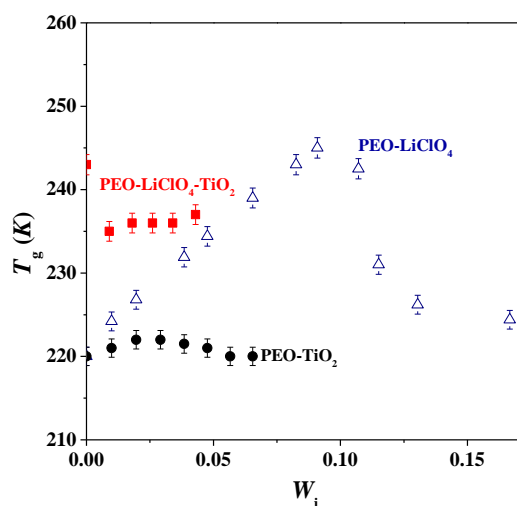


Figure 1. Glass transition temperature of amorphous PEO for (Δ) PEO-LiClO₄, (●) PEO-TiO₂ and (■) PEO-LiClO₄-TiO₂ systems. The error bar represents the standard deviation of the T_g values with an error of less than 3%.

The molecular dispersion of salt in the PEO might be possible due to the complex interaction of salt molecules and PEO segments but it is impossible for the PEO with incorporation of TiO₂ nanofillers. Molecular chains of PEO, as well as the TiO₂, behave like hard spheres to each other as they dislike each other, hence, phase separation takes place in the amorphous phase of PEO. The TiO₂ nanofiller agglomerates and forms micro-particles with an elevating mass fraction of TiO₂ that may lead to severe phase separation [19,20]. Thus, leads to the insignificant difference in T_g for the immiscible system as indicated by the constancy of T_g of PEO with increasing of nanofiller content for PEO-TiO₂ and PEO-LiClO₄-TiO₂ systems.

3.2 Intermolecular Interactions

FTIR is a powerful vibrational spectroscopic method that is widely used to study the intermolecular interactions between components of a polymer mixture [2,60,61]. FTIR is a useful characterization tool as it provides information on the complexation between salt and polymer, nanofiller and polymer, and salt, nanofiller and polymer systems. In general, the shifting in wavenumbers or/and the changes in the intensities of the characteristic absorption peaks of polymer complexes using FTIR give an insight into the interactions that occur between the components of the complex system which may allow one to elucidate the structure of the complex system.

The characteristics of the neat PEO, PEO-LiClO₄, PEO-TiO₂ and PEO-LiClO₄-TiO₂ systems were checked using FTIR. The FTIR analysis is discussed here to highlight the absorption bands of neat PEO, PEO-LiClO₄, PEO-TiO₂ and PEO-LiClO₄-TiO₂ systems. Therefore, the change in the IR absorption bands of PEO upon the addition of salt or nanofiller or salt and nanofiller can be highlighted. Figure 2 shows the full range of FTIR spectra (i.e., wavenumber range from 4000 to 650 cm⁻¹) of neat PEO, PEO-LiClO₄, PEO-TiO₂ and PEO-LiClO₄-TiO₂ systems. The assignment of characteristic IR bands of PEO is based on the previous work by other researchers are listed in Table 2. The characteristic of IR bands of neat PEO in this study is found to be substantially similar to the characteristic IR bands extracted from the literature.

The most important vibrational modes and wavenumbers exhibited by neat PEO are CH₂ bending [ν_s (CH₂)], CH₂ wagging [ω (CH₂)] and C–O–C stretching [ν (C–O–C)] modes. Generally, the characteristic ω (CH₂) mode of PEO shows a sharp doublet at 1360 and 1342 cm⁻¹ representing the crystalline phase of PEO. The centre peak of ν (C–O–C) mode appears as a triplet at 1095 cm⁻¹ that corresponds to the amorphous part of PEO, while the two shoulders represent the crystalline phase of PEO at 1145 and 1060 cm⁻¹, respectively [60].

With the addition of LiClO₄ (i.e., $W_s = 0.0099$) to the PEO matrix, the absorbance bands of PEO show a slight difference in peak wavenumber shifting as compared to the neat PEO. Meanwhile, with incorporation of TiO₂ (i.e., $W_f = 0.0099$) into the PEO matrix reveals that the FTIR spectrum of the PEO-TiO₂ system closely resembles that of the neat PEO except for a little change in the intensities of a few peaks which are peaks of the ν (C–O–C) modes. Besides, the FTIR spectra for PEO-LiClO₄-TiO₂ at $W_s = 0.107$, $W_f = 0.009$ show relatively fewer changes in the wavenumber and peak intensities of the vibrational bands of PEO-LiClO₄-TiO₂ with the addition of nanofiller as compared to PEO-TiO₂ systems. The vibrational modes of CH₂ stretching, CH₂ wagging and C–O–C stretching were shifted to higher wavenumbers. The shape of all CH₂ modes changed with decreased intensity.

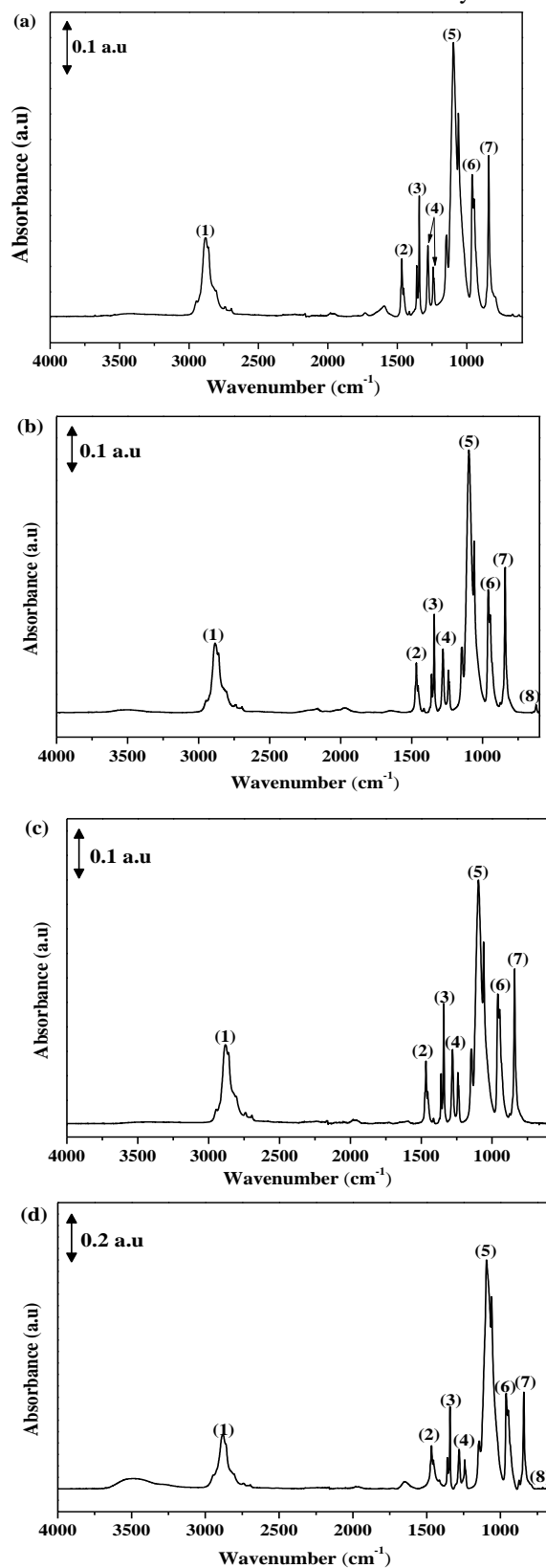


Figure 2. FTIR spectra of (a) neat PEO, (b) PEO-LiClO₄ at $W_S = 0.0099$, (c) PEO-TiO₂ at $W_F = 0.0099$ and (d) PEO-LiClO₄-TiO₂ systems at $W_S = 0.107$, $W_F = 0.009$, respectively.

Figure 3 (a) and (b) show the enlarged view of the absorption bands of CH₂ stretching and CH₂ wagging of PEO-LiClO₄ systems, respectively. The peak intensity at a wavenumber of 1342 and 2884 cm⁻¹ are reduced as the amount of the addition LiClO₄ increasing indicates that the addition of LiClO₄ disrupted the ordering of the polymer chains of PEO and increased the amorphous of PEO [69]. However, the wavenumbers of PEO-LiClO₄ systems at all salt compositions do not shift significantly.

Figure 3 (b) depicts two sharp absorption bands at 1360 and 1342 cm⁻¹ representing the crystalline phase of PEO [60,63–66]. There is no shifting of the wavenumber of the absorbance bands at 1342 cm⁻¹ with the addition of LiClO₄, but the absorbances of these bands reduce as the content of LiClO₄ in the PEO matrix increases, which indicates qualitatively proportionate to the lower content of the crystalline phase in the PEO [70].

Furthermore, another three important absorption IR bands of PEO are also observed to represent C-O-C stretching mode of the band [c.f.

Figure 3 (c)]. The middle peak of $\nu(\text{C-O-C})$ mode observed at 1095 cm⁻¹ corresponds to the amorphous phase of PEO, while the two shoulders representing the crystalline phase of PEO are observed at 1060 and 1148 cm⁻¹ [60,62–65]. There is a slight shifting of absorbance bands of $\nu(\text{C-O-C})$ mode of the amorphous phase of PEO to lower frequency (*i.e.*, from 1095 to 1078 cm⁻¹) and becomes broadened in shape. This is confirmed that there is the interaction between LiClO₄ with the amorphous phase of PEO. As for the shoulders, no clear shifting of the absorbance bands is observed. This is true since the LiClO₄ did not interact with the crystalline region of PEO [19,20]. However, the intensity of the absorbance peak becomes lower upon the addition of LiClO₄.

The band of 623 cm⁻¹ is assigned as the perchlorate “free” anion vibrations (ClO₄⁻) [27,35]. This band is frequently used to analyze ion-ion interactions in PEO-LiClO₄ systems [70]. The $\nu(\text{ClO}_4^-)$ mode of PEO in

Figure 3 (d) shows insignificant shifting in the wavenumber with ascending LiClO₄ content in the PEO matrix implying ions dissociation within the range of the salt content [27]. However, the intensity of the band increases with the increase of the salt content. This may suggest that there is an increment in the amount of free ClO₄⁻ anion or the dissociation of Li cation is also increased. Hence, it is confirmed by FTIR spectra that PEO-LiClO₄ systems have good polymer-salt intermolecular interaction at low salt content but weak polymer-salt intermolecular interaction at high salt content.

Figure 4 illustrates the FTIR spectra of $\omega(\text{CH}_2)$ and $\nu(\text{C-O-C})$ of PEO-TiO₂ systems. The composition of nanofiller is kept low (*i.e.*, $W_F \leq 0.0654$) because TiO₂ starts to agglomerate in the amorphous region of PEO and forms micro-size particles at high composition of nanofiller [19,20,40,71,72]. The doublet of $\omega(\text{CH}_2)$ that represents the crystalline phase of PEO remains unchanged in both position and intensity at all nanofiller compositions [c.f., Figure 4 (a)

and (b)]. This implies that the crystallinity of PEO has no or little interaction with the addition of nanofillers [19,73,74]. Normally, good molecular interactions lead to

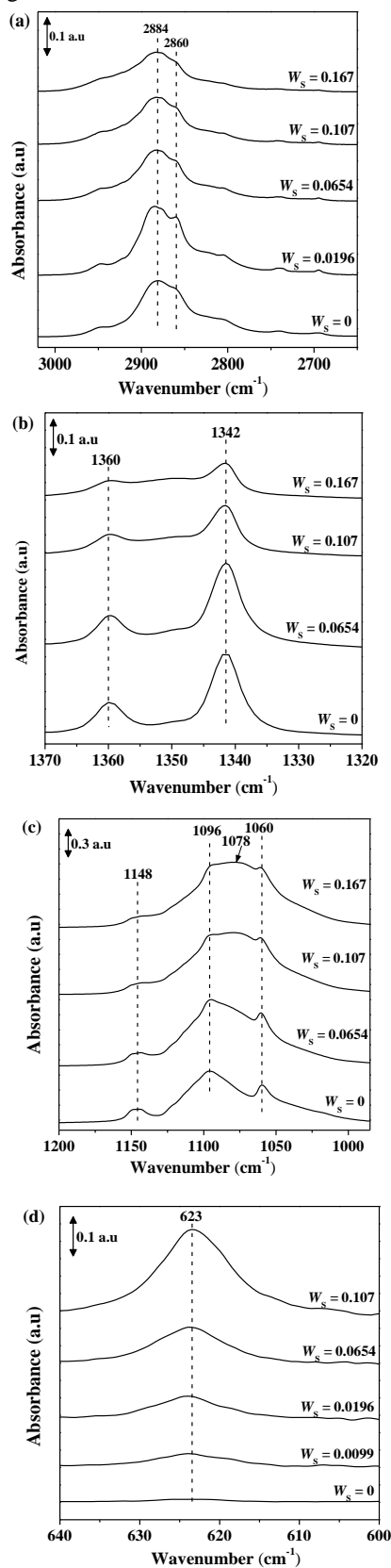


Figure 3. FTIR spectra of (a) CH₂ stretching, (b) CH₂ wagging, (c) C-O-C stretching and (d) ClO₄⁻ of PEO-LiClO₄ systems

largely modifying the shape of the bands and their peak positions [71]. In other words, the PEO matrix is not affected by the addition of TiO₂. However, it can be noted from the enlarged view presented in Figure 4 (c), there are no significant changes neither in intensity nor in positions of the triplet of absorbance bands of $\nu(\text{C-O-C})$ mode at 1060, 1096 and 1147 cm⁻¹ for PEO-TiO₂ systems even increasing the nanofiller content up to $W_F = 0.0654$. These results confirm that there are weak intermolecular interactions between the PEO functional group and TiO₂ in the PEO-nanofiller system because intermolecular interactions significantly alter the shape of the bands and their peak positions [71,75]. In this scenario, the presence of TiO₂ primarily functions as a physical confinement for PEO chains which potentially causes changes in their molecular arrangement and crystalline structures as reported by reference [61,71]. Hence, it is confirmed that the addition of TiO₂ without any surface treatment into the PEO matrix did not have substantial effects on the molecular interaction between PEO and nanofiller in PEO-TiO₂ systems. It serves as a classical model of polymer-nanofiller systems with weak polymer-nanofiller molecular interaction.

The enlarged view of a doublet of $\omega(\text{CH}_2)$ for PEO-LiClO₄-TiO₂ systems at a fixed amount of salt, $W_S = 0.107$ which represents CH₂ stretching and CH₂ wagging are depicted in Figure 5 (a) and (b), respectively. The peak intensity of a doublet of $\omega(\text{CH}_2)$ and their wavenumbers at all nanofiller compositions of PEO-LiClO₄-TiO₂ systems remain unchanged as the amount of TiO₂ increases indicating that the crystalline phase of PEO is unaffected with the addition of nanofiller. In addition, no difference is observed when the addition of TiO₂ as low as $W_F = 0.009$ in PEO-LiClO₄-TiO₂ systems for absorbance bands of $\nu(\text{C-O-C})$ mode where the peak intensity and the wavenumber (*i.e.*, 1094, 1059 and 1146 cm⁻¹) are insignificant changes. Normally, the interactions among PEO, LiClO₄ and TiO₂ are associated with the changes in intensity, shape and position of these stretching modes [70]. Hence, this observation may indicate weaker or no interaction of LiClO₄ and PEO after the addition of TiO₂. However, the loose boundary region may exist at the interface of TiO₂ and PEO. As a result, it may allow the attraction of charged entities to the loose boundary of TiO₂ which possibly helps in the facilitation of the charged entities at the interface of TiO₂ and PEO [76].

Moreover, the band of 623 cm⁻¹ shows an insignificant shift in the wavenumber with an ascending concentration of TiO₂ [*c.f.*, Figure 5 (d)]. This may suggest that there is no significant variation in the amount of free ClO₄⁻ anion or dissociation of Li cation when a small amount of TiO₂ is added. This is due to the charged entities may be attracted more to the loose interfacial region around the surface of TiO₂ [76], thus weakening the interaction of PEO and LiClO₄. Hence, it led to insignificant changes for the free anion and dissociated cation of the PEO-LiClO₄-TiO₂ ternary systems.

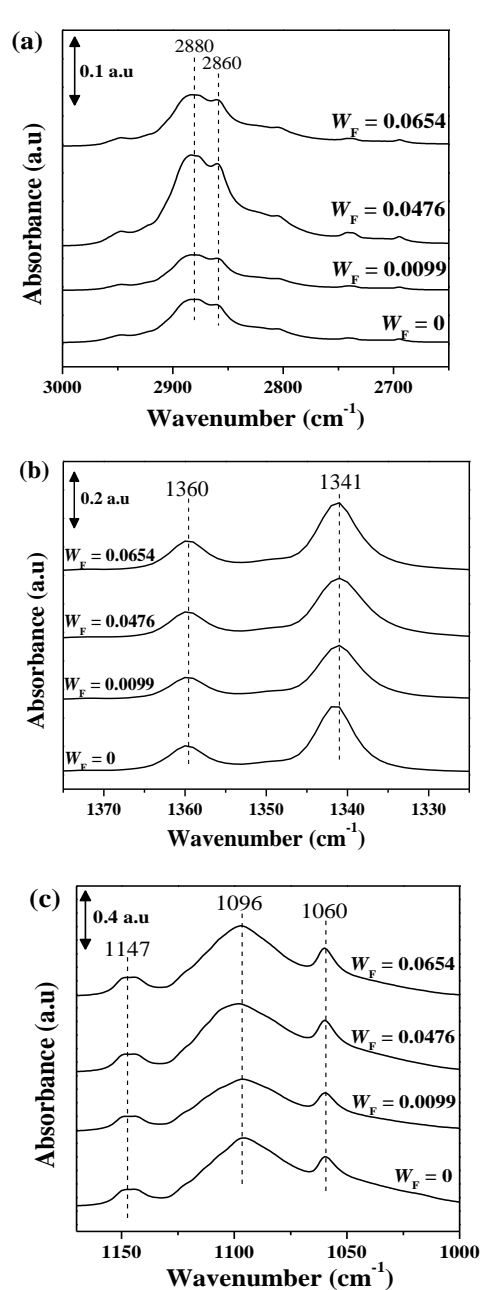


Figure 4. FTIR spectra of (a) CH₂ stretching, (b) CH₂ wagging and (c) C-O-C stretching of PEO-TiO₂ systems

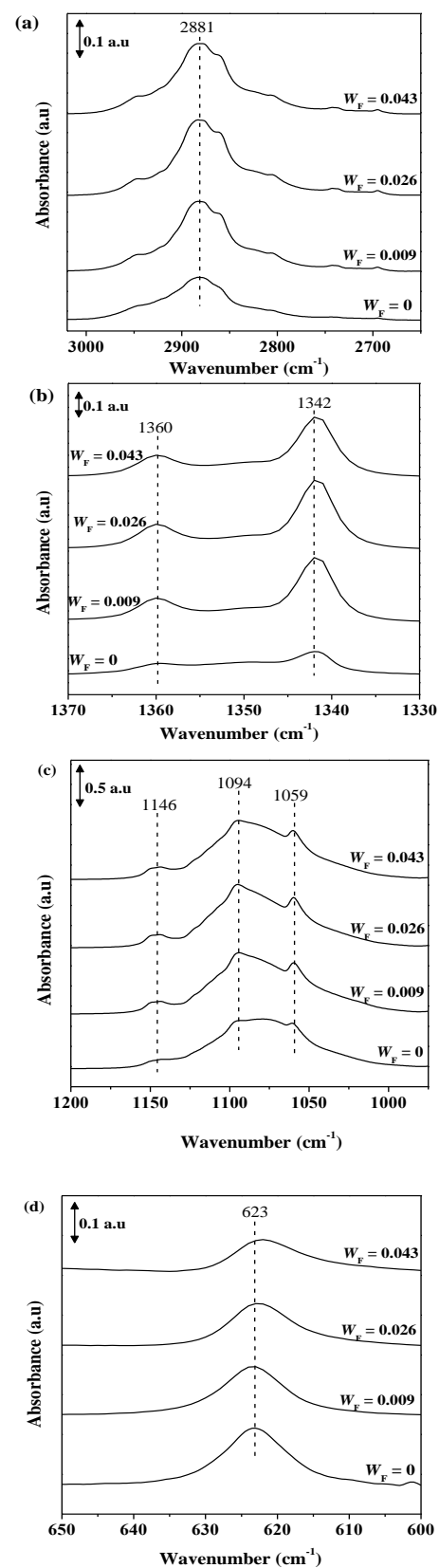


Figure 5. FTIR spectra of (a) CH₂ stretching, (b) CH₂ wagging, (c) C-O-C stretching and (d) ClO₄⁻ of PEO-LiClO₄-TiO₂ systems at fixed salt content, $W_S = 0.107$

Table 2. Characteristics IR bands for neat PEO, PEO-salt, PEO-nanofiller and PEO-salt-nanofiller systems

No	Assignment	Neat PEO		PEO-LiClO ₄ system (W _S = 0.0099)		PEO-TiO ₂ system (W _F = 0.0099)	PEO-LiClO ₄ - TiO ₂ system (W _S = 0.107, W _F = 0.009)
		Wavenumber (cm ⁻¹)	Refs.	Wavenumber (cm ⁻¹)	Refs.	Wavenumber (cm ⁻¹)	Wavenumber (cm ⁻¹)
(1)	CH ₂ stretching, ν_s (CH ₂)	2886	[60,62–64]	2884	[60,62–64]	2880	2881
(2)	CH ₂ scissoring, δ_{as} (CH ₂)	1466	[60,62–64]	1467	[60,62–65]	1466	1466
(3)	CH ₂ wagging doublet, ω (CH ₂)	1342, 1360	[60,63,64,66]	1342, 1360	[60,63–66]	1341, 1360	1342, 1360
(4)	CH ₂ twisting, ω (CH ₂)	1240, 1280	[35,60,63,64]	1240, 1279	[35,60,63–65]	1240, 1281	1240, 1281
(5)	Symmetric C-O-C stretching, ν (C-O-C)]	1060, 1095, 1145	[60,62–64]	1060, 1096, 1148	[60,62–65]	1060, 1096, 1147	1059, 1094, 1146
(6)	CH ₂ symmetric rocking, ρ_s (CH ₂)	962	[35,60,63,64]	961	[35,60,63–65]	961	962
(7)	CH ₂ asymmetric rocking, ρ_{as} (CH ₂)	842	[35,60,64,67]	841	[35,60,64,65,67]	841	842
(8)	ν (ClO ₄ ⁻)	n.a		623	[35,65,68]	n.a	623

4. CONCLUSION

This work focuses on the effect of the addition of salt or/and nanofiller on the T_g and intermolecular interactions of PEO-LiClO₄, PEO-TiO₂ and PEO-LiClO₄-TiO₂ systems. The values of T_g for the amorphous phase of PEO increased with ascending salt content before starting to decrease at a higher salt fraction, $W_S \geq 0.107$. The values of T_g for PEO-TiO₂ and PEO-LiClO₄-TiO₂ systems do not change significantly with an increment of nanofiller fraction. This indicates that there is little or no effect of the addition of TiO₂ to the PEO and PEO-salt systems.

Besides, the FTIR study revealed there is a slight shifting of absorbance bands of asymmetric and symmetric C-O-C stretching mode of the amorphous phase of PEO to lower frequency and becomes broad in shape for PEO-LiClO₄ systems. The peak intensity of the absorption bands of CH₂ stretching and CH₂ wagging of the crystalline phase of PEO reduces as the amount of the addition of LiClO₄ increases which indicates that the addition of LiClO₄ disrupted the ordering of the polymer chains of PEO and increases the amorphous of PEO. However, the

wavenumbers of PEO-LiClO₄ systems at all salt compositions are insignificantly shifting but the absorbances of these bands reduce as the content of LiClO₄ in the PEO matrix increases, which indicates qualitatively proportionate to the lower content of the crystalline phase in the PEO.

Nevertheless, the addition of nanofiller into PEO and PEO-salt systems only has substantial effects on the intermolecular interactions. The absorbance band of asymmetric and symmetric C-O-C stretching, CH₂ stretching and CH₂ wagging modes in terms of the peak intensity and their wavenumbers at all nanofiller compositions of PEO-TiO₂ and PEO-LiClO₄-TiO₂ systems remain unchanged as the amount of TiO₂ increases indicates that the crystalline phase of PEO is unaffected with the addition of nanofiller. Hence, it is confirmed that the addition of TiO₂ without any surface treatment into the PEO matrix did not have substantial effects on the molecular interaction between PEO and nanofiller in PEO-TiO₂ and PEO-LiClO₄-TiO₂ systems. It serves as a classical model of polymer-nanofiller systems with weak polymer-nanofiller molecular interaction. For future prospects, more studies on the surface modifications of TiO₂ are needed to improve the dispersion and interaction with the PEO matrix. Good dispersion and interaction between the TiO₂ filler and PEO

matrix will determine the performance of this composite and their practical applicability.

ACKNOWLEDGEMENTS

The authors sincerely acknowledge the late Prof. Dr. Melissa Chan Chin Han for her endless support and knowledge in this work.

REFERENCES

- [1] M.L. Verma, H.D. Sahu, *Ionics*. **23** (2017) 2339–2350.
- [2] A.R. Polu, H.-W.W. Rhee, *J. Ind. Eng. Chem.* **37** (2016) 347–353.
- [3] B.K. Bahuleyan, C. Induja, M.T. Ramesan, *Polym. Compos.* **40** (2019) 4416–4426.
- [4] Z. Zhao, W. Liang, S. Su, X. Jiang, Y. Bando, B. Zhang, Z. Ma, X. Wang, *Next Mater.* **7** (2025) 100364.
- [5] J. Li, X. Chen, S. Muhammad, S. Roy, H. Huang, C. Yu, Z. Ullah, Z. Wang, Y. Zhang, K. Wang, B. Guo, *Mater. Today Energy* **43** (2024) 101574.
- [6] A.R. Polu, S. Song, A.A. Kareem, S. V. Savilov, P.K. Singh, M. Venkanna, C.S. Kumar, *J. Phys. Chem. Solids* **196** (2025) 112319.
- [7] Y. He, Y. Dong, L. Qiao, C.M. Costa, S. Lanceros-Méndez, J. Han, W. He, *Energy Storage Mater.* **67** (2024).
- [8] D. Liu, X. Liu, L. Zheng, F. Chen, C. Guo, *Polymer*. **313** (2024) 127674.
- [9] S. Kozdra, M. Atsumi, *Mater. Today Commun.* **39** (2024) 109019.
- [10] Z. Li, P. Liu, K. Zhu, Z. Zhang, Y. Si, Y. Wang, L. Jiao, *Energy and Fuels* **35** (2021) 9063–9079.
- [11] J. Gurusiddappa, W.M.R.P. Suvama, K.P. Dasan, *Int. J. Innov. Res. Sci. Eng. Technol.* **4** (2015) 11447–11454.
- [12] R.C. Agrawal, G.P. Pandey, *J. Phys. D. Appl. Phys.* **41** (2008).
- [13] D.K. Pradhan, R.N.P. Choudhary, B.K. Samantaray, *Int. J. Electrochem. Sci.* **3** (2008) 597–608.
- [14] C.H. Chan, L.H. Sim, H.W. Kammer, W. Tan, N.H. Abdul Nasir, *Mater. Res. Innov.* **15** (2011) 2–5.
- [15] H. Ramli, C.H. Chan, A.M.M. Ali, *Macromol. Symp.* **382** (2018) 1–11.
- [16] J. Hu, W. Wang, B. Zhou, Y. Feng, X. Xie, Z. Xue, *J. Memb. Sci.* **575** (2019) 200–208.
- [17] S. Das, A. Ghosh, *AIP Adv.* **5** (2015).
- [18] D.K. Pradhan, R.N.P. Choudhary, B.K. Samantaray, *Mater. Chem. Phys.* **115** (2009) 557–561.
- [19] S.N.H.M. Yusoff, S.I.A. Halim, A.A.A. Tarmizi, N.F.A. Zainal, C.C. Han, *Macromol. Symp.* **408** (2023) 2200065.
- [20] S.N.H.M. Yusoff, S.I.A. Halim, A.A.A. Tarmizi, C.H. Chan, *Polym. Int.* **72** (2023) 935–948.
- [21] D. Zhou, D. Shanmukaraj, A. Tkacheva, M. Armand, G. Wang, *Chem* **5** (2019) 2326–2352.
- [22] S. Choudhary, R.J. Sengwa, *Electrochim. Acta* **247** (2017) 924–941.
- [23] M. Zhu, J. Wu, Y. Wang, M. Song, L. Long, S.H. Siyal, X. Yang, G. Sui, *J. Energy Chem.* **37** (2019) 126–142.
- [24] J.P. Sharma, N. Guleria, *J. Thermoplast. Compos. Mater.* **35** (2022) 1154–1168.
- [25] C.H. Chan, H.W. Kammer, *Ionics*. **22** (2016) 1659–1667.
- [26] A. Arya, A.L. Sharma, *J. Mater. Sci. Mater. Electron.* **29** (2018) 1–29.
- [27] S.I.A. Halim, C.H. Chan, T. Winie, *Macromol. Symp.* **371** (2017) 114–124.
- [28] K. Miguel I. Delgado Rosero; Nori M. Jurado Meneses; Ramiro Uribe, *Materials*. **12** (2019) 1464.
- [29] X. Yu, A. Manthiram, *Energy Storage Mater.* **34** (2021) 282–300.
- [30] H.P.S. Missan, B.S. Lalia, K. Karan, A. Maxwell, *Mater. Sci. Eng. B Solid-State Mater. Adv. Technol.* **175** (2010) 143–149.
- [31] A. Sil, R. Sharma, S. Ray, *Surf. Coatings Technol.* **271** (2015) 201–206.
- [32] S. Choudhary, R.J. Sengwa, *J. Appl. Polym. Sci.* **132** (2015) 1–12.
- [33] D.K. Pradhan, R.N.P. Choudhary, B.K. Samantaray, *Express Polym. Lett.* **2** (2008) 630–638.
- [34] M. Menisha, S.L.N. Senavirathna, K. Vignarooban, N. Iqbal, H.M.J.C. Pitawala, A.M. Kannan, *Solid State Ionics* **371** (2021) 115755.
- [35] L.H. Sim, S.N. Gan, C.H. Chan, R. Yahya, *Spectrochim. Acta - Part A Mol. Biomol. Spectrosc.* **76** (2010) 287–292.
- [36] M. Almakry, *Pure Appl. Sci.* **15** (2016) 24–35.
- [37] C.W. Lin, C.L. Hung, M. Venkateswarlu, B.J. Hwang, *J. Power Sources* **146** (2005) 397–401.
- [38] L. Kratofil Krehula, J. Stjepanović, M. Perlog, S. Krehula, V. Gilja, J. Travas-Sejdic, Z. Hrnjak-Murgić, *Polym. Bull.* **76** (2019) 1697–1715.
- [39] V.T. Nguyen, M. Tabish, G. Yasin, M. Bilal, T.H. Nguyen, C.P. Van, P. Nguyen-Tri, R.K. Gupta, T.A. Nguyen, *Nano-Structures and Nano-Objects* **25** (2021) 100671.
- [40] R.J. Sengwa, S. Choudhary, P. Dhatarwal, *J. Mater. Sci. Mater. Electron.* **30** (2019) 12275–12294.
- [41] M.J. O’Neil, *The Merck Index - An Encyclopedia of Chemicals, Drugs, and Biologicals*, 2013.
- [42] R.J. Seyler, *Assignment of the Glass Transition Temperature*, ASTM International, 1994.
- [43] C.T. Moynihan, M.A. Easteal, Bolt, J. Tucker, *J. Am. Ceram. Soc.* **59** (1976) 12–16.
- [44] S.I. Abdul Halim, C.H. Chan, H.-W. Kammer, *Polym. Test.* **79** (2019) 105994.
- [45] C.B. Roth, J.R. Dutcher, *Eur. Phys. J. E* **12** (2003) 103–107.
- [46] N.S. Hussin, F. Harun, C.H. Chan, *Macromol. Symp.* **376** (2017) 1–7.

- [47] S.I. Abdul Halim, C.H. Chan, J. Apotheker, *Chem. Teach. Int.* **3** (2021) 117–129.
- [48] K.H. Liao, S. Aoyama, A.A. Abdala, C. Macosko, *Macromolecules* **47** (2014) 8311–8319.
- [49] N.F.A. Zainal, H. Ramli, M. Fritz, V. Abetz, C.H. Chan, *Pure Appl. Chem.* **93** (2021) 1119–1139.
- [50] G. Foran, D. Mankovsky, N. Verdier, D. Lepage, A. Prébé, D. Aymé-Perrot, M. Dollé, *IScience* **23** (2020) 1–16.
- [51] S.K. Fullerton-Shirey, J.K. Maranas, *J. Phys. Chem. C* **114** (2010) 9196–9206.
- [52] S.K. Fullerton-Shirey, J.K. Maranas, *Macromolecules* **42** (2009) 2142–2156.
- [53] I.A. Tsekmes, R. Kochetov, P.H.F. Morshuis, J.J. Smit, in: 2013 IEEE Int. Conf. Solid Dielectr., IEEE, 2013, pp. 678–681.
- [54] D.M. Panaitescu, C. Radovici, M. Ghiurea, H. Paven, M.D. Iorga, *Polym. Plast. Technol. Eng.* **50** (2011) 196–202.
- [55] S. Choudhary, R.J. Sengwa, *Polym. Bull.* **72** (2015) 2591–2604.
- [56] S.N.H.M. Yusoff, S.I.A. Halim, N.F.A. Zainal, C.C. Tay, V. Abetz, C.H. Chan, (2024).
- [57] M. Perrier, S. Besner, C. Paquette, A. Vallée, S. Lascaud, J. Prud'homme, *Electrochim. Acta* **40** (1995) 2123–2129.
- [58] S. Besner, J. Prud'homme, *Macromolecules* **22** (1989) 3029–3037.
- [59] A. Ito, P. Phulkerd, V. Ayerdurai, M. Soga, A. Courtoux, A. Miyagawa, M. Yamaguchi, *Polym. J.* **50** (2018) 857–863.
- [60] S.I.A. Halim, C.H. Chan, L.H. Sim, *Macromol. Symp.* **365** (2016) 95–103.
- [61] P. Utpalla, S.K. Sharma, K. Sudarshan, V. Kumar, P.K. Pujari, *Eur. Polym. J.* **117** (2019) 10–18.
- [62] N.H. Gondaliya, D.K. Kanchan, P. Sharma, P. Joge, *Mater. Sci. Appl.* **02** (2011) 1639–1643.
- [63] T. Yoshihara, H. Tadokoro, S. Murahashi, *J. Chem. Phys.* **41** (1964) 2902–2911.
- [64] Y.L. Ni'Mah, M.Y. Cheng, J.H. Cheng, J. Rick, B.J. Hwang, *J. Power Sources* **278** (2015) 375–381.
- [65] S. Jayanthi, K. Kulasekarapandian, A. Arulsankar, K. Sankaranarayanan, B. Sundaresan, *J. Compos. Mater.* **49** (2015) 1035–1045.
- [66] C. Manoratne, R.M.G. Rajapakse, M.A.K.L. Dissanayake, *Int. J. Electrochem. Sci.* (2006).
- [67] H. Matsuura, T. Miyazawa, *J. Polym. Sci. Part A-2 Polym. Phys.* **7** (1969) 1735–1744.
- [68] B. Jinisha, A.F. Femy, M.S. Ashima, S. Jayalekshmi, *Mater. Today Proc.* **5** (2018) 21189–21194.
- [69] J. Ji, B. Li, W.H. Zhong, *Electrochim. Acta* **55** (2010) 9075–9082.
- [70] A. Dey, S. Karan, S.K. De, *J. Phys. Chem. Solids* **71** (2010) 329–335.
- [71] P. Dhatarwal, S. Choudhary, R.J. Sengwa, *Polym. Bull.* **78** (2021) 2357–2373.
- [72] G. Toskas, C. Cherif, R.D. Hund, E. Laourine, A. Fahmi, B. Mahltig, *ACS Appl. Mater. Interfaces* **3** (2011) 3673–3681.
- [73] S. Ketabi, K. Lian, *Electrochim. Acta* **154** (2015) 404–412.
- [74] F. Harun, C.H. Chan, T. Winie, *Polym. Int.* **66** (2017) 830–838.
- [75] R.J. Sengwa, P. Dhatarwal, *Electrochim. Acta* **338** (2020) 135890.
- [76] S.I.A. Halim, N.F.A. Zainal, C.H. Chan, J. Kressler, *Pure Appl. Chem.* **95** (2023) 755–777.